

DIRECT OBSERVATION OF LOW CORONAL BREAKOUT: DOES BREAKOUT PRECEDE OR FOLLOW SOLAR ERUPTION?

SU-CHAN BONG,¹ Y.-J. MOON,¹ K.-S. CHO,¹ YEON-HAN KIM,¹ Y. D. PARK,¹ AND G. S. CHOE²

Received 2005 October 19; accepted 2005 November 30; published 2006 January 3

ABSTRACT

In this Letter, we report a direct *SOHO* LASCO C1 observation of low coronal “magnetic breakout” that occurred during the coronal mass ejection (CME) on 1998 March 23. The LASCO C1 images show that a slowly expanding, small coronal loop on the northeastern limb erupted, becoming a CME with the typical three-part structure (core, void, and front). Just after the CME front went out of the C1 field of view (about 2 solar radii), a wedgelike open structure is clearly formed. From this observation, together with *Yohkoh* SXT and *SOHO* MDI images, we inferred the change of the coronal magnetic field configuration during the eruption, which shows a morphological consistency with the breakout CME model. However, our observation shows that the initial acceleration ($\sim 100 \text{ m s}^{-2}$) of the CME front began about 1 hr before the apparent field opening. This observation disagrees with the CME initiation mechanism of the breakout model. We note that the observed eruption progressed in four distinct phases: a slow rise of loop structures, the initial acceleration of the CME, the magnetic breakout and second acceleration, and the CME propagation at almost-constant speed.

Subject headings: Sun: corona — Sun: coronal mass ejections (CMEs) — Sun: magnetic fields

1. INTRODUCTION

The solar eruption is quite a global phenomenon, which comprises different observational features such as a flare, an eruptive prominence, and a coronal mass ejection (CME). The eruption springs from a closed magnetic field configuration in quasi-static equilibrium, in which the upward magnetic pressure force of the low-lying sheared (or twisted) field and the downward tension force of the overlying quasi-potential field are more or less balanced. At the onset of an eruption, part of the nonpotential magnetic flux and the plasma contained within it are expelled from the Sun. For this to happen, the catastrophic removal of the overlying field (i.e., field opening) is essential (Hundhausen 1999).

A total field opening had been regarded as energetically impossible according to the Aly-Sturrock theorem (Aly 1991; Sturrock 1991). Since the applicability of this theorem to real solar eruptions is quite limited (see Forbes 2000; Choe & Cheng 2002), most CME theories thereafter tried to work around it. Among the many CME models proposed so far (e.g., Forbes 2000; Low 2001; Lin et al. 2003), the breakout model (Antiochos 1998; Antiochos et al. 1999) has turned out to be a successful attempt to explain the removal of the overlying field barrier without contradiction of the Aly-Sturrock theorem. This model assumes a quadrupolar (or more complex) field geometry. The magnetic field to erupt initially lies under the overlying field, which runs almost antiparallel to the former, and is energized by a shearing (twisting) motion or the emergence of new flux. The expansion of the underlying field creates a current sheet between the underlying and overlying flux systems. Reconnection in this current sheet transfers the reconnected fluxes to the sidelobe flux systems. After enough of the overlying flux is reconnected with part of the underlying flux, the apex of some field lines in the underlying flux system can go out of the observing window, and this process can be ob-

served as field opening within the observational field of view. Thus, the field opening in the breakout model may well be called “virtual” opening.

So far several observational studies have been put forward in support of, or consistent with, the breakout model (Aulanier et al. 2000; Sterling & Moore 2001, 2004a, 2004b; Wang et al. 2002; Manoharan & Kundu 2003; Maia et al. 2003; Pohjolainen et al. 2005). However, there has been no direct observation of breakout of the overlying field. In this Letter, we report an eruptive event showing “breakout” of the coronal field observed in *Solar and Heliospheric Observatory (SOHO)* Large Angle Spectrometric Coronagraph (LASCO; Brueckner et al. 1995) C1 Fe xiv images and compare our observation with recent numerical simulations of the breakout model (Lynch et al. 2004; MacNeice et al. 2004).

2. OBSERVATIONS

Figure 1 shows the negative images of LASCO C1 Fe xiv (*top row*) and *Yohkoh* Soft X-ray Telescope (SXT; Tsuneta et al. 1991) Al/Mg filter images (*bottom row*) at four different times. As shown in the C1 images, a loop-shaped structure, indicated by arrows, rapidly expanded and went out of the field of view. In the second column, we can clearly see its three-part structure: core, void, and front. Just after the CME front escaped from the C1 field of view (about 2 solar radii), we note an wedgelike open structure (*third column*). Comparing two images taken at 00:21 and 00:51 UT, it is evident that this open structure resulted from the expulsion of the CME loop. The wedge-shaped open configuration lasted for about 3 hr until 03:53 UT and slowly narrowed over the following several hours (*last column*).

The images in the first column in Figure 1 were taken just after the onset of a noticeable eruptive behavior. In the C1 image (*top panel*), we can see a loop structure, indicated by the arrows, overlying a bright core. The position of this core is quite close to that of the X-ray loop seen in the SXT image (*bottom panel*). Considering the time gap between the C1 and SXT images, we can assume that the bright core of the C1 image corresponds to the X-ray loop.

Before the fast eruption, there had been slow rising motions

¹ Korea Astronomy and Space Science Institute, 61-1 Hwaam-dong, Yuseong-gu, Daejeon 305-348, South Korea; scbong@kasi.re.kr, yjmoon@kasi.re.kr, kscho@kasi.re.kr, yhkim@kasi.re.kr, ydpark@kasi.re.kr.

² Princeton Plasma Physics Laboratory, Princeton, NJ 08543-0451; gchoe@pppl.gov.

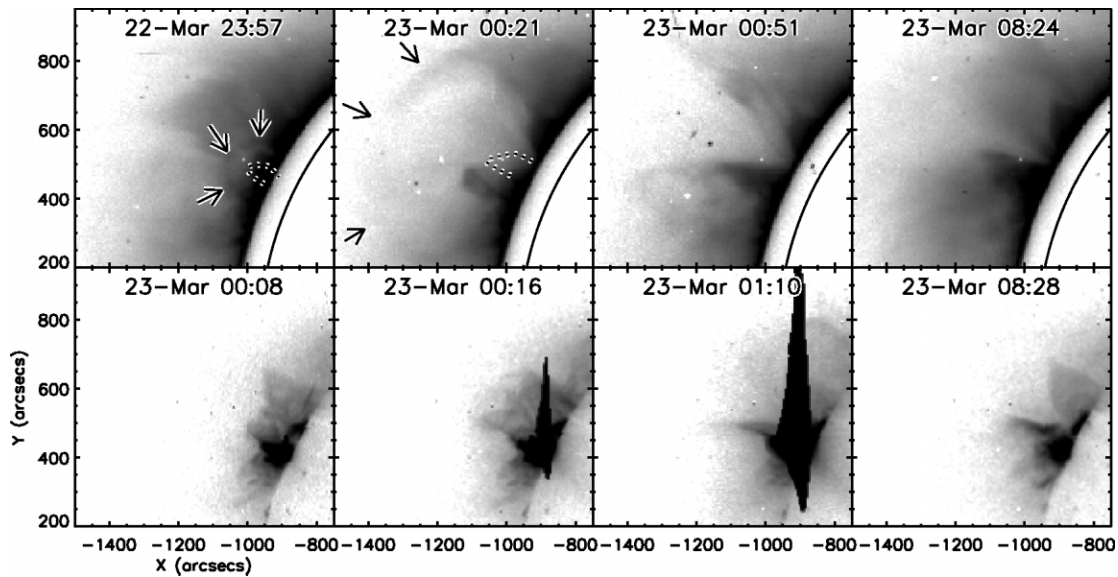


FIG. 1.—SOHO LASCO C1 (top row) and Yohkoh SXT (bottom row) negative images showing eruption. The arc in the lower right corner of each C1 image represents the solar limb. Arrows indicate the erupting Fe XIV (C1) loop. The dotted line overlaying the C1 images (top row) contours the erupting X-ray (SXT) loop seen in the bottom row.

in both structures for several hours. Figure 2a shows the height versus time profiles of the CME and X-ray loops. In the figure, we can see slow rising motions of both the CME and X-ray loops from 19:00 to 23:30 UT, before the onset of a fast eruption. The rising speed is estimated to be around 1 km s^{-1} .

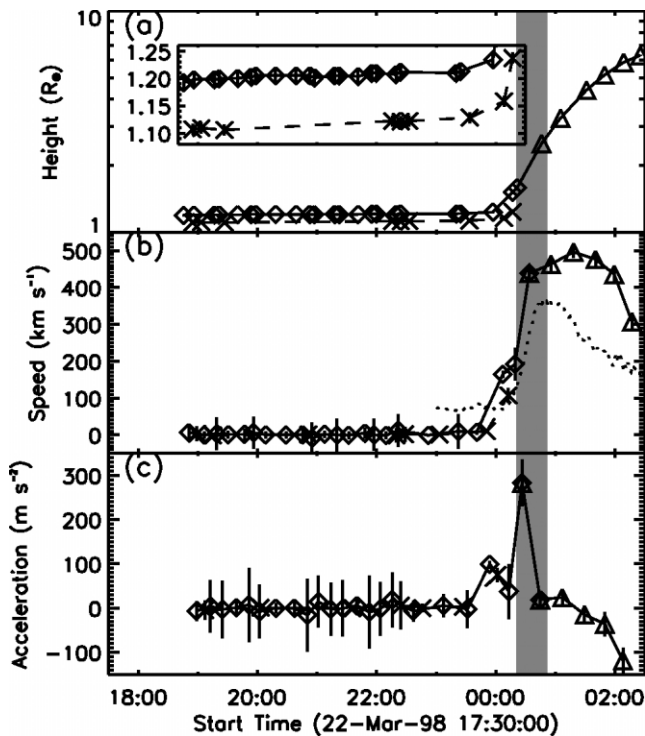


FIG. 2.—(a) Height, (b) speed, and (c) acceleration of the CME (solid line) and the X-ray loop (dashed line). The inset in (a) is a magnified view of the early slow-rise phase. The CME heights are measured from C1 (diamonds) and C2 (triangles) images, and the X-ray loop heights (crosses) from SXT images. The measurement error is assumed to be 2 pixels in each image. In most cases, error bars are smaller than the symbol size. The speed is calculated from the altitude difference between two consecutive observing times. The dotted line in (b) shows the maximum brightness temperature in NoRH 17 GHz images in arbitrary units. The field opening occurred at a time within the gray zone.

A remarkable acceleration signifying a fast eruption began between 23:24 and 23:57 UT for the CME front and the core. We cannot precisely tell which structure was accelerated earlier than the other; however, considering their coherent rising behaviors up to $\sim 00:00$ UT, their simultaneous onsets can be speculated. After 00:00 UT, the CME front proceeded faster than the X-ray loop or the CME core, increasing the difference in their altitudes (compare the first and second columns of Fig. 1). The acceleration of the CME front persisted for more than 1 hr and ended near 00:30 UT. Thereafter, the CME front propagated at a constant speed and even decelerated (Figs. 2b and 2c).

In the second SXT image of Figure 1 (also in Nobeyama Radioheliograph [NoRH] images, not shown here), we can see a small flare below the ejected X-ray loop. The flare was so weak that we could not find any significant enhancement in the GOES X-ray flux. The SXT brightening started with the X-ray loop acceleration between 23:33 and 00:08 UT and peaked at 01:10 UT. However, due to the observational gap before 01:10 UT, its actual peak could be timed much earlier than that. The microwave brightening in NoRH images began at 00:11 UT, slightly later than the X-ray brightening and reached a maximum at 00:49 UT, probably right after the apparent field opening. A summary of the observed incidents of importance is given in Table 1.

Examining a series of SXT movies, we found that the remaining X-ray structure did not change much for several days after the eruption. Figure 3a and 3b show the SXT image and

TABLE 1
SUMMARY OF OBSERVED INCIDENTS

Time (UT)	Incident
19:00–23:24	Slow rise of Fe XIV (C1) and X-ray (SXT) loops
23:24–23:57	Start of Fe XIV (C1) loop fast eruption
23:33–00:08	Start of X-ray (SXT) loop fast eruption and brightening
00:11	Start of microwave (NoRH) brightening
00:21–00:52	Fe XIV (C1) field opening
00:49	Microwave (NoRH) brightening maximum
01:10	X-ray (SXT) brightening maximum
03:50	End of microwave (NoRH) brightening
03:53–10:00	Fe XIV (C1) open field narrowing

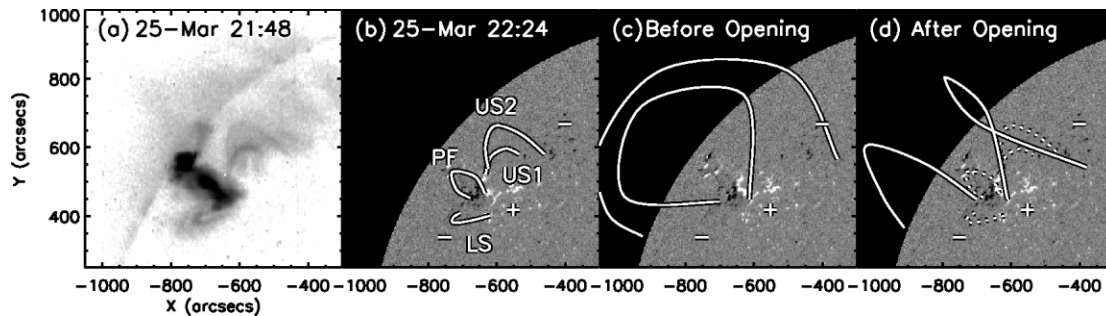


FIG. 3.—Observed and speculated magnetic field configuration. (a) The SXT negative image and (b) the *SOHO* MDI magnetogram are both taken about 3 days after the eruption. The positive and negative field regions are colored in white and black and marked with plus and minus signs, respectively. The X-ray loop connectivities obtained from (a) are drawn in white lines over the magnetogram in (b). Coronal field connectivities (c) before (March 23 00:21 UT) and (d) after (00:51 UT) the field opening are inferred from the C1 images and the magnetogram. The schematic field lines are drawn over the same magnetogram in (b). Dotted lines in (d) are the same field lines drawn in (b).

the *SOHO* Michelson Doppler Imager (MDI; Scherrer et al. 1995) magnetogram taken about 3 days after the event. In Figure 3b, we can see that there are three (one positive and two negative) different magnetic polarity areas, between which one can draw two polarity-inversion line segments. Field line connectivities (US1, US2, PF, and LS in the figure) overlaid in the MDI images are deduced from the comparison of visible SXT loops and magnetic polarities. The bright, central post-flare loop (PF), over which the eruption occurred, and the lower side loop (LS) connect from the central positive zone to the lower negative zone, but these two loops are neither nested nor parallel. The upper side loops (US1 and US2) connect from the central positive zone to the upper negative zone.

3. INTERPRETATION AND DISCUSSION

Based on the X-ray loop field connectivity and the C1 images, we project the coronal field connectivity over the X-ray structures just before and after the formation of the wedge-like configuration in Figures 3c and 3d. At 00:51 UT, just after the apparent field opening, we can imagine a slightly skewed, large coronal loop overlying the X-ray upper side loops (US1 and US2), and another loop starting from east of the post-flare loop (PF) and ending in a positive polarity zone somewhere behind the limb (see Fig. 3d). The valley formed between these two loops is seen as an open wedge structure. Before the field opening at 00:21 UT, we can make two nested, bulged loop structures (Fig. 3c), whose magnetic fields run almost antiparallel, by reconnecting those two coronal loops in Figure 3d backward in time. According to this field connectivity interpretation, the global magnetic field configuration of this event was essentially quadrupolar, which is one of main elements of the breakout CME model. The reconnection progressing from Figure 3c to 3d is nothing but a breakout process. Therefore, we examine our observations in view of the breakout model (Antiochos 1998) and its recent numerical simulations (Lynch et al. 2004; MacNeice et al. 2004).

The long and slow rise before the eruption well agrees with the original scenario of the breakout model, in which this is explained by the gradual increase of magnetic shear in the central flux system. The start time of the CME acceleration, however, is contradictory to the conceptual breakout model and the simulations. According to the simulation by Lynch et al. (2004), the acceleration allegedly begins with the reconnection at the overlying null point. However, our observation has shown that the apparent field opening (magnetic breakout) occurred near the end of the acceleration. A plausible explanation is that the main acceleration mechanism in this event is not the mag-

netic breakout, although a breakout occurred in the course of the eruption as an aftermath of the initial acceleration. In response to this argument, we propose a two-stage acceleration scenario. In fact, a careful examination of the speed profiles of the LASCOS C1 and C2 loops (Fig. 2) reveals that there are two strong acceleration phases, the first at 23:53 UT and the second at 00:26 UT. The second acceleration exactly coincides with the breakout time.

According to the breakout simulation model (Lynch et al. 2004), the central magnetic flux is transferred to the sidelobes during eruption, and the reconnection of the central open field creates the flare impulsive phase. Therefore, the X-ray flare is supposed to start after the acceleration caused by breakout, and its brightness is expected to reach a maximum after the apparent field opening. While the observed timing of the X-ray flare start is earlier than the model timing, the timing of the SXT brightness maximum falls a while after the field opening, as the model suggests. From all the above observational results, it can be inferred that the breakout was not caused by energization of the coronal field by interaction between the inner and outer bipolar fields, but by another catastrophic eruptive process in the lower corona, possibly involving magnetic reconnection. In this regard, we note that in the simulation by MacNeice et al. (2004), the flare reconnection apparently drives the breakout reconnection more than the latter drives the former, while admitting that the two reconnection processes facilitate each other.

It is interesting to note that the wedge-shaped open field structure remains quasi-stable for about 3 hr, from 01:00 to 04:00 UT. This time span is almost coincident with that of the microwave brightening in the NoRH images. The persistence of the open field structure for such a long time after the eruption is quite peculiar and is difficult to understand in terms of the breakout model, or perhaps any other known models.

4. SUMMARY AND CONCLUSION

We have presented a solar eruption observed by *SOHO* LASCOS C1 and *Yohkoh* SXT. The C1 images show a typical three-body structure (core, void, and front) even several hours before the eruption. The bright core in C1 is seen as an X-ray loop in SXT images. The pre-eruptive slow rise ($\sim 1 \text{ km s}^{-1}$) continued for several hours for both the front and the core, which is similar to previous observations (e.g., Ohya & Shibata 1998; Sterling & Moore 2004a, 2004b). They started to be accelerated almost simultaneously within the time cadence of the data. The acceleration of the CME front lasted about 1 hr and then the front propagated with an almost constant

speed ($\sim 500 \text{ km s}^{-1}$). The acceleration had two phases, and the second one was coincident with the apparent opening of the magnetic field in the C1 field of view. The wedge-shaped open structure remained quasi-stable for about 3 hr, and then the angle of the wedge got smaller over the following several hours.

Based on the MDI magnetogram and the X-ray loop structures obtained a few days afterward, we found that the evolution of the magnetic field configuration agrees with the breakout model. However, the initial acceleration preceded the apparent field opening in our observation, which disagrees with the initiation mechanism of the breakout model. The observed CME kinematics indicate that the eruption was initiated by another mechanism, not by breakout. As for the quasi-stable, open structure lasting as long as 3 hr, we also cannot find a satisfactory explanation in existing CME models.

In summary, the overall progress of this eruption comprises four distinct phases: the slow rise before the eruption, the initial acceleration, the magnetic breakout and second acceleration, and the propagation of the CME. (1) In the slow-rise phase, the coronal loop and the underlying core slowly rise, probably due to the increase of magnetic shear or emergence of new flux. (2) In the initial acceleration phase, the coronal loop and the core

are accelerated up to 200 km s^{-1} with a peak acceleration of $\sim 100 \text{ m s}^{-2}$. (3) In the breakout and second acceleration phase, the magnetic field apparently opens up in the field of view and the CME is accelerated up to 500 km s^{-1} with a peak acceleration of $\sim 300 \text{ m s}^{-2}$. (4) In the propagation phase, the CME proceeds in the interplanetary space along with solar wind. The initial acceleration mechanism remains unknown, but it may be related to a near-surface activity (such as pre-eruptive reconnection), because the dynamics of the X-ray loop is almost consonant with that of the CME loop in C1 images.

The authors greatly appreciate the referee's constructive comments. This work was supported by the Ministry of Science and Technology (MOST) grants (M1-0104-00-0059 and M1-0407-00-0001) and the Korea Research Foundation (KRF-2005-070-C00059) of the Korean government. G. S. C. was supported by DoE contract DE-AC02-76-CH0-3073 and NASA grant NNH04AA161. The *SOHO* LASCO data used here are produced by a consortium of the Naval Research Laboratory (US), Max-Planck-Institut für Sonnensystemforschung (Germany), Laboratoire d'Astronomie (France), and the University of Birmingham (UK). *SOHO* is a project of international cooperation between ESA and NASA.

REFERENCES

- Aly, J. J. 1991, *ApJ*, 375, L61
 Antiochos, S. K. 1998, *ApJ*, 502, L181
 Antiochos, S. K., DeVore, C. R., & Klimchuck, J. A. 1999, *ApJ*, 510, 485
 Aulanier, G., DeLuca, E. E., Antiochos, S. K., McMullen, R. A., & Golub, L. 2000, *ApJ*, 540, 1126
 Brueckner, G. E., et al. 1995, *Sol. Phys.*, 162, 357
 Choe, G. S., & Cheng, C. Z. 2002, *ApJ*, 574, L179
 Forbes, T. G. 2000, *J. Geophys. Res.*, 105, 23153
 Hundhausen, A. J. 1999, in *The Many Faces of the Sun*, ed. K. Strong et al. (New York: Springer), 143
 Lin, J., Soon, W., & Baliunas, S. L. 2003, *NewA Rev.*, 47, 53
 Low, B. C. 2001, *J. Geophys. Res.*, 106, 25141
 Lynch, B. J., Antiochos, S. K., MacNeice, P. J., Zurbuchen, T. H., & Fisk, L. A. 2004, *ApJ*, 617, 589
 MacNeice, P. J., Antiochos, S. K., Phillips, A., Spicer, D. S., DeVore, C. R., & Olson, K. 2004, *ApJ*, 614, 1028
 Maia, D., Aulanier, G., Wang, S. J., Pick, M., Malherbe, J.-M., & Delaboudinière, J.-P. 2003, *A&A*, 405, 313
 Manoharan, P. K., & Kundu, M. R. 2003, *ApJ*, 592, 597
 Ohya, M., & Shibata, K. 1998, *ApJ*, 499, 934
 Pohjolainen, S., Vilmer, N., Khan, J. I., & Hillaris, A. E. 2005, *A&A*, 434, 329
 Scherrer, P. H., et al. 1995, *Sol. Phys.*, 162, 129
 Sterling, A. C., & Moore, R. M. 2001, *ApJ*, 560, 1045
 ———. 2004a, *ApJ*, 602, 1024
 ———. 2004b, *ApJ*, 613, 1221
 Sturrock, P. A. 1991, *ApJ*, 380, 655
 Tsuneta, S., et al. 1991, *Sol. Phys.*, 136, 37
 Wang, T., Yan, Y., Wang, J., Kurokawa, H., & Shibata, K. 2002, *ApJ*, 572, 580